High-Yield Functional Expression of Human Sodium/D-Glucose Cotransporter1 in *Pichia pastoris* and Characterization of Ligand-Induced Conformational Changes as Studied by Tryptophan Fluorescence†

Navneet K. Tyagi,‡ Pankaj Goyal,§ Azad Kumar,‡ Dharmendra Pandey,§ Wolfgang Siess,§ and Rolf K. H. Kinne*,‡

Department of Epithelial Cell Physiology, Max Planck Institute of Molecular Physiology, Otto-Hahn Strasse 11, 44227, Dortmund, Germany, and Institute for Prevention of Cardiovascular Disease, Ludwig Maximilian University, Pettenkoferstrasse 9, 80336, Munich, Germany

Received July 15, 2005; Revised Manuscript Received September 22, 2005

ABSTRACT: Studies on the structure−function relationship of transporters require the availability of sufficient amounts of the protein in a functional state. In this paper, we report the functional expression, purification, and reconstitution of the human sodium/D-glucose cotransporter1 (hSGLT1) in *Pichia pastoris* and ligand-induced conformational changes of hSGLT1 in solution as studied by intrinsic tryptophan fluorescence. hSGLT1 gene containing FLAG tag at position 574 was cloned into pPICZB plasmid, and the resulting expression vector pPICZB-hSGLT1 was introduced into *P. pastori*s strain GS115 by electroporation. Purification of recombinant hSGLT1 by nickel-affinity chromatography yields about 3 mg of purified recombinant hSGLT1 per 1-liter of cultured *Pichia* cells. Purified hSGLT1 migrates on SDS−PAGE with an apparent mass of 55 kDa. Kinetic analysis of hSGLT1 in proteoliposomes revealed sodium-dependent, secondary active, phlorizin-sensitive, and stereospecific α-methyl-D-glucopyranoside transport, demonstrating its full catalytic activity. The position of the maximum intrinsic tryptophan fluorescence and titration with hydrophilic collisional quenchers KI, acrylamide, and trichloroethanol suggested that most of Trps in hSGLT1 in solution are in a hydrophobic environment. In the presence of sodium, sugars that have been identified earlier as substrate for the transporter increase intrinsic fluorescence in a saturable manner by a maximum of 15%. α-Methyl-D-glucopyranoside had the highest affinity (K_d = 0.71 mM), followed by D-glucose, D-galactose, D-mannose, and D-allose which showed a much lower affinity. L-Glucose was without effect. D-Glucose also increased the accessibility of the Trps to hydrophilic collisional quenchers. On the contrary phlorizin, the well-established inhibitor of SGLT1, decreased intrinsic fluorescence by a maximum of 50%, and induced a blue shift of maximum (5 nm). Again, the effects were sodium-dependent and saturable and a high affinity K_d of 5 μM was observed. In addition the surface of hSGLT1 was labeled with 1-anilinonaphthalene-8-sulfonic acid, a reporter molecule for the surface hydrophobicity. In the presence of sodium, addition of D-glucose decreased ANS fluorescence whereas phlorizin increased ANS fluorescence. Thus three conformational states of SGLT1 could be defined which differ in their packing density and hydrophobicity of their surface. They reflect properties of the empty carrier, the D-glucose loaded carrier facing the outside of membrane and the complex of the outside-orientated carrier with phlorizin.

To survive and function properly, cells exchange substances such as nutrients, ions, and metabolites with their environment. These tasks are performed by transporter proteins that are embedded in the cell membrane. Membrane proteins account for 30% of the human genome (*1*), are involved in a wide spectrum of hereditary and somatic disorders and diseases from cancer to infertility, and are targets of more than 50% of the drugs currently used in therapeutics. A majority of these transport proteins use either ion or solute gradients as the driving force to translocate substrates across the membrane, and they are called secondary active transporters. An important example of this class is the human Na^+/glucose cotransporter1 (hSGLT1[1]), which is responsible for the accumulation of sugars in the epithelial cells of intestine and kidney (*2*, *3*). Mutations in hSGLT1 lead to the glucose/galactose malabsorption syndrome (*4*).

Heterologous expression of hSGLT1 has been described in *Xenopus laevis* oocytes (*2*), COS-7 cells (*5*), Sf9 cells (*6*), CHO cells (*7*) and *Escherichia coli* (*8*) and has increased our knowledge about the function of the transporter signifi-

† This work was supported by funds of the International Max Planck Research School in Chemical Biology.

* To whom correspondence should be addressed. E-mail: rolf.kinne@mpi-dortmund.mpg.de. Tel: +49 (0) 231-133 2200. Fax: +49 (0) 231-133 2299.

‡ Max Planck Institute of Molecular Physiology.

§ Ludwig Maximilian University.

[1] Abbreviations: hSGLT1, human sodium/D-glucose cotransporter1; D-Glu, D-glucose; Phlz, phlorizin; PCR, polymerase chain reaction; BMGY, buffered glycerol-complex medium; BMMY, buffered methanol-complex medium; LB, Luria Bertani medium; YPD, yeast extract peptone dextrose medium; α-MDG, α-methyl-D-glucopyranoside; Trp, tryptophan; KI, potassium iodide; TCE, trichloroethanol; ANS, 1-anilinonaphthalene-8-sulfonic acid.

10.1021/bi051377q CCC: $30.25
Published on Web 11/02/2005

cantly. The amount of protein produced in the above-mentioned systems is, however, not sufficient for most of the biochemical, biophysical, or structural studies which require some times up to hundreds of milligrams of highly purified protein. In view of these difficulties our group previously concentrated on the expression and purification of different functional domains of SGLT1 (*9*, *10*). Their subsequent use as a model for the identification of a phlorizin-binding site and an alkyl glucoside-binding site as studied by fluorescence spectroscopy and affinity labeling (*9*−*12*) provided valuable information about the mechanism of action of different inhibitors.

However, there remains still an urgent need to express hSGLT1 in full-length and in sufficient quantities. To achieve high-level expression of hSGLT1 we chose to use the methyltropic yeast *Pichia pastoris* because in the last 15 years this expression system has emerged as most successful for the heterologous expression of a wide variety of foreign proteins (*13*−*16*). This holds especially for membrane proteins whose expression was not possible in *E. coli* or, if it was possible, the protein was expressed in low amounts and often with loss of function. The following membrane proteins have been successfully expressed in *P. pastoris:* Na^+, K^+-ATPase (*17*), multidrug resistance protein1 (*18*), ATP-binding cassette transporter (*19*), NOP-1 (*20*), mammalian intestinal peptide transporter (*21*), human μ-opioid receptor (*22*), and $5HT_{5A}$-serotoninergic receptor (*23*).

The mechanism by which SGLT1 transport the substrates across the cell membrane is still unknown. A commonly proposed model is that cotransport results from ligand-induced conformational transitions (*24*) that change the accessibility of ligand-binding sites from one side of the membrane to the other. These conformational changes in hSGLT1 are poorly understood. We describe here the expression of full-length hSGLT1 in methylotropic yeast *P. pastoris* and demonstrate its functional integrity by transport studies in *P. pastoris* membrane vesicles and proteoliposomes. Furthermore we studied its intrinsic and extrinsic fluorescence properties in solution to characterize substrate and inhibitor induced conformational changes of cotransporter.

EXPERIMENTAL PROCEDURES

Materials. The *P. pastoris* strains (pPICZB, GS115), *E. coli* strain (TOP10F'), Zeocin, and all media (LB, YPD, BMGY, and BMMY) were from Invitrogen (Carlsbad, CA). Restriction enzymes *Eco*RI, *Xho*I, *Not*I, and *Pme*I were from New England Biolabs (Frankfurt am Main, Germany). All PCR reagents were from Stratagene (Amsterdam, The Netherlands). α-Methyl-D-[^{14}C] glucopyranoside ([^{14}C] α-MDG) was from Perkin-Elmer LAS (Rodgau-Jügesheim, Germany). All sugars, phlorizin, asolectin soy lecithin, cholesterol, and 2,2,2-trichloroethanol were from Sigma (Munich, Germany). All other chemicals were of analytical grade and obtained from commercial sources.

Construction of Expression Vector pPICZB-hSGLT1. The full-length hSGLT1 containing clone (DKFZp686N20230Q2) was purchased from Deutsches Ressourcenzentrum für Genomforschung GmbH (RZPD, Berlin, Germany). cDNA coding of hSGLT1 was amplified by polymerase chain reaction using the following primer: sense, 5′-TATTGAATTCGATGGACAGTAGCACCTG-3′, and antisense, 5′-AATACTCGAGGGCAAAATATGCATGGC-3′ containing *Eco*RI and *Xho*I restriction sites. For better immunological detection and to provide ease in the purification process, the FLAG epitope was introduced in hSGLT1 by changing the native peptide sequence D_{574} AEEEN to D_{574}YKDDDDK. For this modification the following primer sequences were used: 5′-GACGACGATAAGATCCAACAAGGCCCTAAGGAGAC-3′ and 5′-ATCCTTGTAATCCAGGTCAATACGCTCCTCTTTGC-3′ (*25*). After all these modifications in cDNA of hSGLT1, this modified cDNA was amplified by PCR reaction using two synthetic oligonucleotides: sense, 5′-TATTGAATTCAAAATGGACAGTAGCACCTG-3′, and antisense, 5′-ATTATTGCGGCCGCGGCAAAATATGCATGCC-3′, containing *Eco*RI and *Not*I restriction sites.

The PCR product was cloned into *Eco*RI and *Not*I sites of pPICZB vector to obtain hSGLT1 fused with 6× His tag at C-terminal. The resulting pPICZB-hSGLT1 plasmid was transformed into TOP10F′ *E. coli* cells for further propagation and purification of plasmid. All DNA manipulations were performed as described (*26*), and all constructs were verified by DNA sequencing.

Electroporation of P. pastoris with Plasmid pPICZB or pPICZB-hSGLT1. The purified DNA samples of pPICZB and pPICZB-hSGLT1 were linearized by *Pme*I digestion at 37 °C for 3 h, and the linearized plasmids DNA were purified by enzyme removal column.

YPD medium (100 mL) was inoculated in a 1-liter flask with 0.2 mL of overnight culture of *P. pastoris* strain GS115, and the cells were grown at 28 °C overnight to an OD_{600} of 2−4. Overnight grown culture was centrifuged at 1500*g* at 4 °C for 5 min. The supernatant was removed and the pellet was resuspended with 25 mL of ice-cold sterile water. The resuspended cells were centrifuged again as above, and the pellet was resuspended in 8 mL of ice-cold sterile 1 M sorbitol. The cells were centrifuged as above, and then the pellet was resuspended with 1 mL of ice-cold sterile 1 M sorbitol. The suspension of competent cells was kept on ice and used the same day.

The suspensions of competent cells (40 μL) and of linearized DNA (10 μL, 10 μg) were mixed and transferred to an ice-cold electroporation cuvette. The cuvette with the mixture of cells and DNA was incubated on ice for 5 min. The cells were pulsed at 1.5 kV, 50 μF, and 200 Ω, and 1 mL of ice-cold 1 M sorbitol was added to the cuvette. The cuvette contents were transferred to a sterile 15 mL tube and incubated at 30 °C without shaking for 2 h. 200 μL of these cells were plated on YPD medium with 100, 500, and 1000 μg/mL Zeocin and incubated at 30 °C for 2 days.

Protein Expression in P. pastoris. In pilot experiments, single colonies of transformed cells were used to inoculate 2.5 mL of BMGY medium (1% (w/v) yeast extract, 2% (w/v) peptone, 100 mM potassium phosphate, pH 6.0, 1.34% (w/v) yeast nitrogen base, 4×10^{-5}% (w/v) biotin, and 1% (v/v) glycerol). After 30−36 h of incubation at 28 °C, the cells were pelleted at 1000*g* and were resuspended in BMMY medium (BMGY medium in which the glycerol was replaced by 1% (v/v) methanol) to induce protein expression. The positive colonies for recombinant protein expression were identified by Western blot analysis by using anti-FLAG antibody (Sigma). The clone with the highest protein yield was selected for medium scale protein expression in 2-liter

flasks. In all subsequent preparations, the cells were harvested at ~24 h of methanol induction.

Membrane Preparation for Transport Studies. Cells cultured in BMMY medium were harvested at OD_{600} of 4−6/mL by centrifugation at 3000*g* at 4 °C for 10 min, washed once with ice-cold breaking buffer (50 mM sodium phosphate, pH 7.4, 10% glycerol), and resuspended in breaking buffer supplemented with protease inhibitor cocktail. An equal volume of acid-washed chilled glass beads (0.5 mm diameter) was added to the suspension, and cells were disrupted by vigorous vortexing 10 times for 1 min, with intervening 1 min incubations on ice. Unbroken cells were removed by centrifugation at 2000*g* at 4 °C for 5 min. Membranes were pelleted at 100000*g* at 4 °C for 30 min and resuspended in membrane suspension buffer (100 mM mannitol, 20 mM HEPES-Tris, pH 7.4) with protease inhibitor cocktail. Aliquots were snap-frozen and stored at −80 °C. The protein concentration of the membrane preparation was determined by using a micro-BCA kit (Pierce, Rockford, IL).

Protein Purification from P. pastoris. Membranes were prepared from *P. pastoris* cells as described in the membrane preparation section. Peripheral proteins and proteins adhering to the membrane were removed by washing with 4 M urea in breaking buffer containing protease inhibitor cocktail (Roche) at 4 °C for 2 h, and the resulting membranes were centrifuged at 100000*g* at 4 °C for 40 min. The stripped membranes were solubilized in buffer TG [20 mM Tris. Cl, pH 8/1 M NaCl/20% (v/v) glycerol] supplemented by 1.2% FosCholine-12 (Anatrace, Maumee, OH) and protease inhibitor cocktail, and the resulting membrane solution was shaken at 4 °C, overnight. After removal of the insoluble fraction by ultracentrifugation at 100000*g* for 40 min at 4 °C, the clear supernatant was bound to the preequilibrated Protino Ni 2000 prepacked (Macherey-Nagel) polyhistidine-tag purification column at 4 °C, and unbound proteins were removed by washing with 3 column volumes of buffer TG plus 0.2% FosCholine-12. Recombinant hSGLT1 was eluted with 9 mL of buffer TG plus 0.2% FosCholine-12 supplemented with 250 mM imidazole and protease inhibitor cocktail. The purified protein containing fractions were concentrated to 0.35 mL by ultrafiltration in Centricon YM100 devices (Millipore) and stored at −20 °C for further use in TG buffer containing 0.2% FosCholine-12.

Reconstitution of Recombinant hSGLT1. Proteoliposomes were prepared using Triton X-100 destabilized liposomes (*27*−*29*). Liposomes were composed of 9:1 asolectin soy lecithin and cholesterol. 10 mg cholesterol and 90 mg asolectin soy lecithin were dissolved in 5 mL of chloroform in a beaker. The solvent was evaporated under a stream of argon to obtain a thin layer of dry lipids. The last traces of solvent were removed under vacuum in a desiccator overnight. Before each reconstitution the lipids were suspended in 5 mL of 100 mM potassium phosphate, pH 7.5/2 mM β-mercaptoethanol to yield a lipid concentration of 20 mg/mL and subsequently sonicated in argon atmosphere in a tip probe sonicator (until the suspension became slightly clear), and the resulting liposomes were stored in liquid nitrogen. Triton X-100 was added at concentrations corresponding to the onset and or total solubilization of lipids as determined by turbidity measurements (*30*). Detergent-destabilized liposomes were mixed with purified protein in a 400:1 (w/w) and incubated at room temperature under gentle agitation for 10 min. Detergent was removed by adding Bio-Beads SM-2 activated according to ref *31* at a wet weight beads:detergent ratio of 6:1. After 1 h of incubation at room temperature, fresh Bio-Beads were added, and incubation was continued for an additional hour. After the third addition of Bio-Beads, incubation was continued overnight at 4 °C. Bio-Beads were removed by filtration on glass silk. Proteoliposomes were concentrated by centrifugation at 300000*g* for 45 min at 4 °C and stored in liquid nitrogen. Proteoliposome pellets for sugar uptake assay were resuspended in 100 mM potassium phosphate/2 mM β-mercaptoethanol (pH 7.5) for final protein concentration of 0.1 μg/mL.

Transport Assay of hSGLT1 in Membranes and in Proteoliposomes. Sugar uptake by right-side-out membrane vesicles was performed as described for *E. coli* right-side-out membrane vesicles (*25*, *27*). Proteoliposomes (preloaded with 100 mM potassium phosphate, pH 7.5/2 mM β-mercaptoethanol) were subjected to three sonication/freeze/thaw cycles before uptake assays at 22 °C. Uptake was initiated by mixing 10 μL of proteoliposomes with 10 μL of transport buffer 2X (200 mM choline/Cl, 50 mM NaCl, 100 mM mannitol, 20 mM Tris, 20 mM HEPES, 300 mM KCl, 6 mM $MgSO_4$, 2 mM $CaCl_2$) with α-methyl-D- [^{14}C] glucopyranoside ([^{14}C] α-MDG). Each reaction was stopped with 1 mL of ice-cold stop solution (10 mM Tris, 10 mM HEPES, 100 mM mannitol, 150 mM KCl, 50 mM choline/Cl, 50 mM NaCl, 3 mM $MgSO_4$, 1 mM $CaCl_2$, 0.2 mM phlorizin), applied centrally to a 0.22 μm nitrocellulose filter GSWP (Millipore) over vacuum and washed with 3 mL of ice-cold stop solution, and the filter was assayed by scintillation counting. All experiments were performed at least in triplicate, and errors indicate the SE of the mean values.

Analytical Methods. Silver staining and Coomassie Blue staining were performed after protein separation by SDS−PAGE using 10% acrylamide gels as described (*32*, *33*). Specific detection of hSGLT1 in cells and extract were achieved by Western blot analysis by using the following antibodies: murine cell culture anti-FLAG M2 monoclonal antibody peroxidase conjugate (Sigma, Munich, Germany), mouse anti-his-tag (27E8) monoclonal antibody (Cell signalling, Baverly, MA), and rabbit anti-human SGLT1 antibody (Acrirs antibodies, Hiddenhausen, Germany).

Steady-State Fluorescence Studies. Steady-state fluorescence measurements were done with a Perkin-Elmer LS 50B fluorescence spectrometer (Perkin-Elmer), fitted with a 450 W xenon arc lamp at room temperature. A 0.3-cm excitation and emission path length quartz cell was used for all the fluorescence measurements. The excitation wavelength was set at 295 nm for selective excitation of Trp. A 290 nm cutoff filter was used to minimize the contribution of scattering signals. Emission spectra were collected from 300 to 400 nm, averaging six scans. The bandwidths for both excitation and emission monochromators were 5 nm. The emission spectra were corrected for the background and dilution effects. All the fluorescence experiments were carried out in PBS (pH 7.3) buffer. The final concentration of protein was 0.016 nM; Fos-Choline-12 was present in a concentration of 0.18 mM.

Quenching of Intrinsic Protein Fluorescence. Potassium iodide (KI), acrylamide, and trichloroethanol (TCE) depend-

ent fluorescence quenching experiments were performed in PBS (pH 7.3) for the hSGLT1 in the absence and presence of 10 mM D-Glucose or 100 μM phlorizin. Increasing concentrations of the quencher were added from a concentrated stock solution of the quencher in the buffer. The accessibility of Trp was monitored by analyzing the quenching data using a Stern−Volmer equation: $F_0/F = 1 + K_{SV}$ [Q], where F_0 is the fluorescence of the protein in the absence of quencher and F is the observed fluorescence at the concentration [Q] of the quencher. K_{SV} is the collisional quenching constant, which was determined from the slope of best-fit values of Stern−Volmer plots at a given concentration of D-glucose or phlorizin. The difference between inner filter effects of substrate (50 μM) from the titration of L-Trp (5 μM) performed at an excitation of 295 nm and emission at 355 nm was found to be very low and hence is not considered in our measurements.

Ligand Binding Assay. The ligand-induced fluorescence changes as a function of D-glucose (D-Glu), D-galactose (D-Gal), 2-deoxy-D-glucose (2Doglc), D-mannose (Man), D-allose (All), L-glucose (L-Glc), or phlorizin (Phlz) concentration was monitored as described (*9*). For the determination of apparent binding constant increasing amounts of sugars (0.1−10 mM) or phlorizin (2−140 μM) were added to hSGLT1 (4.0 μg/mL) in PBS. Apparent binding constants for sugars and phlorizin were calculated by the equation $v/V_{max} = [S]^n/[S]^n + K$, written as below in the form of fluorescence change,

$$\Delta F/\Delta F_{max} = [S]^n/[S]^n + K \quad (1)$$

where [S] is the external substrate (sugars or phlorizin) concentration, ΔF_{max} is the maximal change in fluorescence intensity for saturating [S], K is the binding constant, and n is the Hill coefficient.

ANS Fluorescence. ANS is a naphthalene dye that is strongly quenched by water and undergoes a dramatic increase in fluorescence intensity when it binds to hydrophobic regions of proteins. Solution of ANS was prepared in PBS buffer from 5 mM stock solution in ethanol. The final concentration of ANS was calculated considering the 4950 cm^{-1} M^{-1} (350 nm) extinction coefficient value for ANS in water (*34*). Since the binding of ANS was found to be not instantaneous, ANS and hSGLT1 were incubated for 10 min before the extrinsic fluorescence measurements were made at equilibrium. For the fluorescent probe ANS, excitation wavelength was 370 nm, and emission spectrum was collected in the range of 420−580 nm. The protein and ANS concentrations were 0.016 nM and 100 μM, respectively. All extrinsic fluorescence measurements of ANS labeled hSGLT1 were performed in PBS (pH 7.3) buffer.

RESULTS

Construction of pPICZB-hSGLT1 Expression Vector. The cDNA coding for the human sodium/glucose cotransporter1 (hSGLT1) was cloned into the plasmid pPICZB. In the resulting expression vector pPICZB-hSGLT1 the hSGLT1 gene was under the transcriptional control of the *AOX*1 promoter, which is inducible by methanol. The plasmid was linearized by digestion with *Pme*I, used to transform *P. pastoris* strain GS115, and transformants were selected at low, medium, and high concentrations of Zeocin (100, 500, or 1000 μg/mL). Recombinant derivates of plasmid pPICZB linearized by digestion with *Pme*I typically integrate at the *AOX* locus as a single copy, but multiple copy integration occurs with a frequency of 1 to 10%. Resistance to higher levels of Zeocin correlates with higher copy number for the integrated plasmid, which usually (*35*) but not always (*36*) correlates with higher levels of expression of recombinant protein of interest. In our case clones selected on 1000 μg/mL Zeocin gave the highest yield of hSGLT1 as judged by Western blot analysis by anti-FLAG antibody (data not shown), thus for further expression we used the clone of this plate. The clone with the highest protein yield was grown in BMGY medium supplemented by 100 μg/mL Zeocin for 30−36 h at 28 °C to an OD_{600} of 2−4/mL and then transferred to methanol containing medium (BMMY with 100 μg/mL Zeocin) to induce protein expression for 24 h.

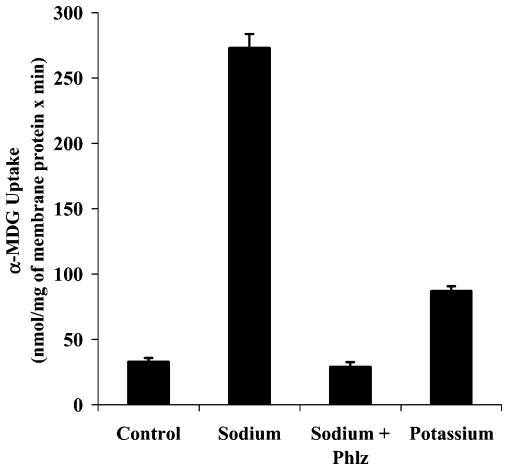

FIGURE 1: Sugar uptake by plasma membrane vesicles of *P. pastoris* expressing hSGLT1. α-MDG (50 μM) uptake by right-side-out vesicles of *P. pastoris* GS115 producing hSGLT1 is stimulated by sodium (Na^+, 100 mM) and inhibited by phlorizin (Phlz, 100 μM). For the control vesicles (plasma membrane vesicles from *P. pastoris* harboring the empty plasmid), there is no significant difference in sugar uptake in the presence or absence of Na^+; transport is also not affected by the addition of phlorizin.

Functional Analysis of Recombinant hSGLT1 in P. pastoris Plasma Membranes. Transport studies in the *P. pastoris* plasma membranes provided first evidence for the expression of functionally active hSGLT1. As shown in Figure 1 in membrane vesicles derived from a transformed strain α-MDG in the presence of a sodium gradient uptake at a rate of 273 ± 11 nmol × mg of membrane $protein^{-1}$ × min^{-1} is observed, which is completely blocked by phlorizin (29 ± 4 nmol × mg of membrane $protein^{-1}$ × min^{-1}). No such phenomenon is observed in membrane vesicles obtained from nontransformed cells (Figure 1).

Purification of hSGLT1 from P. pastoris. A representative purification is shown in Figure 2. The membrane fraction obtained by high-speed ultracentrifugation was washed with 4 M urea to remove peripheral membrane proteins. All SGLT1 remained membrane-bound after this procedure (Figure 2B, lane UW). The stripped membranes were then solubilized in 1.2% FosCholine-12 in TG buffer at 4 °C overnight, and the nonsolubilized material was removed by high-speed centrifugation. The clear supernatant was applied to a preequilibrated Protino Ni-resin column. The protein eluted by using buffer TG with 250 mM imidazole showed an apparent molecular weight of 55 kDa, which corresponds

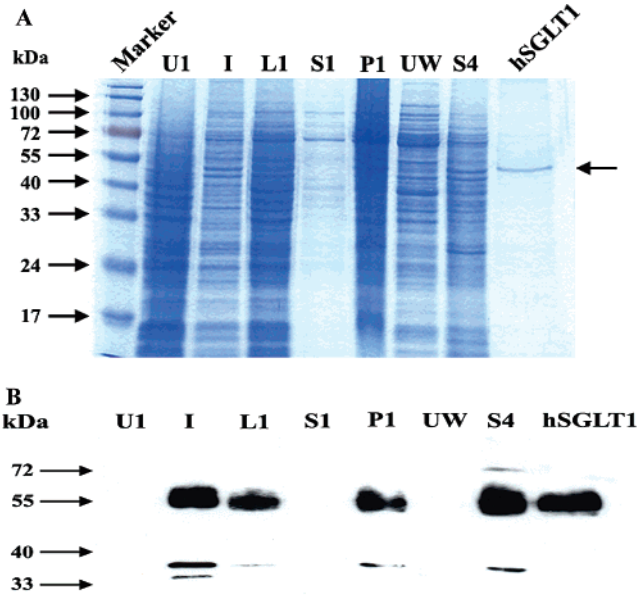

FIGURE 2: Coomassie-stained SDS−PAGE gel and immunoblot of it with anti-FLAG antibody during different stages of hSGLT1 purification. (A) Marker, molecular weight protein marker; UI, uninduced sample; I, induced sample after induction by 1% methanol; L1, whole cell lysate after lysis of *P. pastoris* cells expressing hSGLT1; S1, supernatant; P1, pellet after high-speed centrifugation; UW, washing obtained after 4 M urea wash of pellet P1; S4, supernatant obtained after solubilization of urea wash pellet in 1.2% FosCholine-12; and hSGLT1, Protino column purified hSGLT1 which shows an apparent molecular mass of 55 kDa (marked by arrow). (B) Western blot of above-mentioned SDS−PAGE gel with anti-FLAG antibody.

to the nonglycosylated form of the transporter (Figure 2A, lane hSGLT1), and is recognized by anti-FLAG antibody (Figure 2B), by anti-hSGLT1 and anti-His tag antibodies (data not shown). As judged by Coomassie staining (Figure 2A, lane hSGLT1) and silver staining (data not shown) the protein was more than 95% pure. 1-Liter culture of *P. pastoris* yielded about 3 mg of purified protein.

Functional Analysis of Recombinant hSGLT1 in Proteoliposomes. For reconstitution of purified hSGLT1, preformed liposomes made of 9:1 asolectin soy lecithin and cholesterol were used. The time course of α-MDG uptake into the proteoliposomes in the presence and absence of 100 mM Na^+, and in the presence of 100 μM phlorizin, is shown in Figure 3A. In the presence of 100 mM Na^+, sugar transport peaked within 30 min at 313 ± 13 nmol of α-MDG per mg of recombinant hSGLT1 before falling to the concentration equilibrium of about 60 nmol of α-MDG per mg of recombinant hSGLT1 in more than 5 h time. The time course of α-MDG uptake in proteoliposomes demonstrated a classical overshoot (*37*, *38*) in the presence of Na^+, indicating that sugar was concentrated within the proteoliposomes and that uptake was energized by the electrochemical gradient of Na^+ via secondary active cotransport. The overshoot is absent if there is no sodium gradient across the membrane. These findings indicate a coupling of sodium flux to glucose flux.

The sugar selectivity of recombinant hSGLT1 in proteoliposomes was measured by determining the uptake of 100 μM α-MDG in the presence of 10 mM D-glucose (D-Glc), D-galactose (D-Gal), D-mannose (Man), D-allose (All), L-glucose (L-Glc), and 100 μM phlorizin (Phlz) in the presence

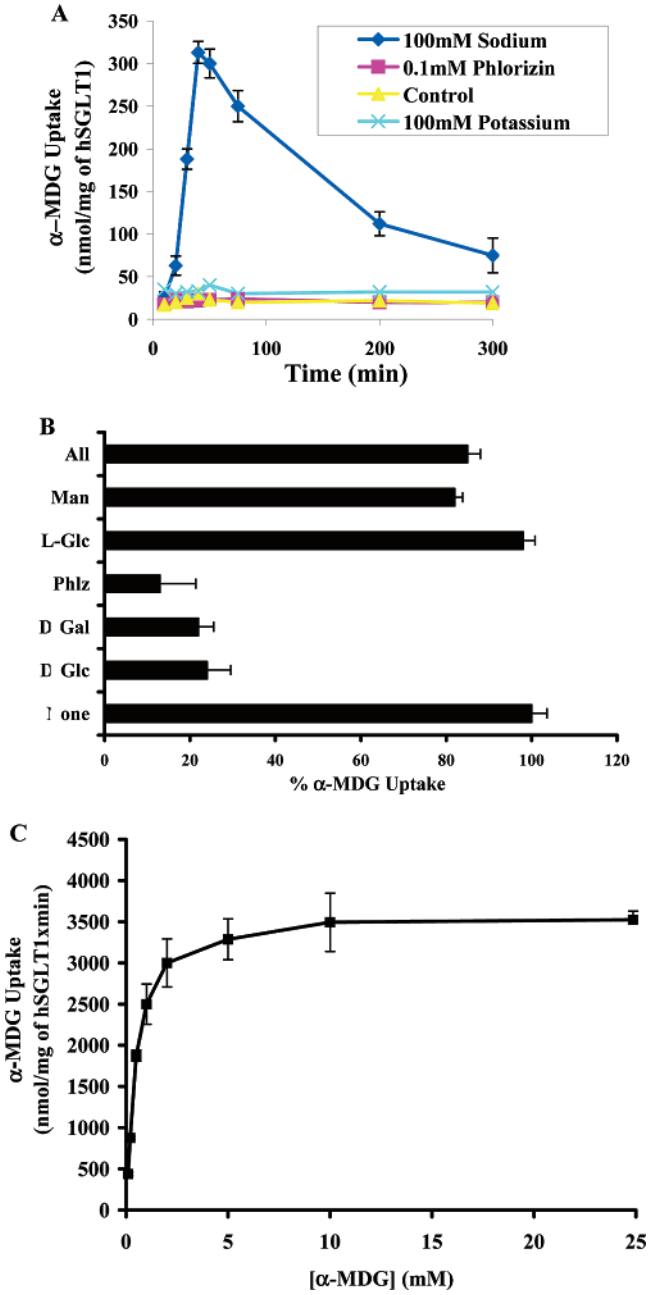

FIGURE 3: Sugar uptake kinetics of proteoliposomes containing purified recombinant hSGLT1. (A) The time course of α-MDG (10 μM) in the presence of 100 mM sodium (◆) shows a 16-fold increase in the initial rate of sugar uptake before reaching concentration equilibrium in 5 h. After addition of 100 μM phlorizin (■) or removal of Na^+ (×), the initial rate is identical to control liposomes containing no hSGLT1 (▲) and sugar accumulation above the equilibrium is not observed. (B) Effect of various substrates and inhibitors on the uptake of α-MDG into proteoliposomes containing purified recombinant hSGLT1. Uptake of α-MDG (100 μM) after 1 min is inhibited by high-affinity substrates or inhibitors of hSGLT1 (10 mM D-glucose, D-Glc; 10 mM D-galactose, D-Gal; 100 μM phlorizin, Phlz) but not by low-affinity substrates (e.g., 10 mM D-mannose, Man; 10 mM D-allose, All; 10 mM L-glucose, L-Glc). (C) Concentration-dependence of the sugar uptake after 1 min shows a half-saturation constant (K_m) of 0.4 ± 0.05 mM/L and maximum velocity (V_{max}) of 3.4 ± 0.34 μmol × mg hSGLT1^{-1} × min^{-1}.

of 100 mM Na^+. D-Glc and D-Gal inhibited Na^+-dependent α-MDG by 75% and 78%, while Man, All, and L-Glc inhibited sugar uptake only by 18%, 15%, and 2%, respec-

Table 1: Effect of Various Substrates and Inhibitors on the Uptake of 100 μM α-MDG after 1 min by Proteoliposomes Containing Purified hSGLT1

substrate/ inhibitor	changes	concn used	% inhibition of α-MDG uptake
none	none	100 μM	0
α-MDG	CH_3 group at C-1	10 mM	95
D-Glu	no CH_3 group at C-1	10 mM	75
D-Gal	axial OH group at C-4	10 mM	78
Man	axial OH group at C-2	10 mM	18
All	axial OH group at C-3	10 mM	15
L-Glu	L-isomer of glucose	10 mM	2
Phlz	phloretin moiety at C-1 position	100 μM	84

tively. In the presence of 100 μM phlorizin the Na^+-dependent sugar uptake was reduced to 84% of the original value (Figure 3B, Table 1). Thus hSGLT1 in proteoliposomes exhibits substrate specificity in the following order: α-MDG > D-Glc ≈ D-Gal ≫ Man > All. Recombinant reconstituted hSGLT1 shows also stereospecificity as it preferred D-Glu over L-Glu: D-Glu inhibited 75% α-MDG uptake, and L-Glu inhibited only 2%.

The sugar selectivity of the reconstituted recombinant hSGLT1 appears to be similar to that reported for the transporter in different systems (*8*, *37*−*40*). The equatorial orientation of the OH-group at the positions C-2 and C-3 of the D-glucose seems to be important for its recognition by hSGLT1 since in the presence of D-mannose and D-allose no significant inhibitory effect on α-MDG uptake was observed. The 78% inhibition of α-MDG uptake in the presence of D-galactose indicates that the orientation of OH-group at C-4 (equatorial in D-glucose and axial in D-galactose) is not that important for recognition by the cotransporter because D-Glu and D-Gal inhibited sugar uptake about equally (Table 1).

For the determination of kinetic parameters, 1 min α-MDG uptake assays were performed at varying α-MDG concentrations from 0.01 to 25 mM. A half-saturation constant (K_m) of 0.4 ± 0.05 mM/L and a maximum velocity (V_{max}) of 3.4 ± 0.34 μmol × mg hSGLT1^{-1} × min^{-1} was observed (Figure 3C). The carrier catalytic turnover number (*41*, *42*), an index of number of sugar molecules transported per transporter, was calculated by dividing the sugar transport V_{max} by the total number of transporters present in the proteoliposomes. Catalytic turnover of hSGLT1 based on the V_{max} of 3.4 μmol × mg hSGLT1^{-1} × min^{-1} is 6 s^{-1}.

Ligand-Induced Changes in Tryptophan Fluorescence. The intrinsic Trp fluorescence of hSGLT1in solution, the effect of sugars on the intrinsic fluorescence, and the accessibility to collisional quenchers are depicted in Figure 4. The fluorescence of the intrinsic Trp residues in hSGLT1 shows an emission maximum at 338−340 nm. Addition of D-glucose, but not L-glucose, increased fluorescence significantly by 13 ± 1% with no shift in the fluorescence maximum. As evident from Figure 4B this increase was concentration dependent. When saturation kinetics were applied an apparent binding affinity of 0.84 ± 0.15 mM could be determined. As summarized in Table 2 also α-methyl-D-glucopyranoside and D-galactose increased the fluorescence whereas D-mannose and D-allose had minor effects.

In Figure 4D and Table 3 experiments are summarized in which the effect of D-glucose on the quenching of the fluorescence by hydrophilic external quenchers of various size was investigated. In the absence of D-glucose a rather low quenching was observed, which is also reflected in the small Stern−Volmer constant. When D-glucose at saturating concentration was present in the medium, the Trp quenching significantly increased. In the presence of D-glucose the Stern−Volmer constants of all the collisional quenchers increased by about 20%. All the effects could only be observed in the presence of sodium, suggesting a link to the sodium−sugar cotransport function of the protein.

These results demonstrate that most of the Trps responsible for the hSGLT1 fluorescence are located within a hydrophobic environment probably buried within the protein. Sugars apparently change the conformation of hSGLT1 in such a way that some Trps move to positions where they become more accessible to external collisional quenchers.

Effect of Phlorizin on the Intrinsic Fluorescence and the Accessibility to Collisional Quenchers. As depicted in Figure 4A, phlorizin, quite in contrast to D-glucose, decreased the intrinsic fluorescence of hSGLT1 in a concentration of 100 μM by about 50%. As shown in Figure 4C this effect increased with the concentration of phlorizin; using saturation kinetics an apparent binding constant of 5 μM was observed. In addition, phlorizin shifted the maximum of the fluorescence by 5 nm to a lower wavelength. In the titration experiments with the collisional quenchers a slight tendency for a decreased accessibility of Trps was observed (Figure 4D, Table 3). Thus phlorizin binding induces a conformation of hSGLT1 that is quite different from that assumed by the transporter when it interacts with D-glucose.

Characterization of Different Conformational States of hSGLT1 by ANS Fluorescence. In order to further study conformational changes in hSGLT1 during substrate/inhibitor carrier interaction, hydrophobic patches on the surface of the protein were labeled with ANS and its fluorescence was measured under various conditions. The emission maximum of ANS bound to hSGLT1 was located at around 488 nm (Figure 5). Addition of D-glucose decreased ANS fluorescence by 10 ± 2% with red shift of 2 nm, suggesting a more hydrophilic environment of some of the ANS molecules. The binding of phlorizin increased the ANS fluorescence by 30 ± 4% with blue shift of 7 nm, which indicates that after interaction with phlorizin the transporter assumes a more compact hydrophobic conformation. Thus changes in conformation deduced from the measurements of the intrinsic Trp fluorescence are also detectable on the surface of protein.

DISCUSSION

Expression and Purification of hSGLT1. For the expression of hSGLT1 various heterologous expression systems have been used, but major disadvantages associated with these systems are that modified proteins are frequently not trafficked properly to the plasma membrane (*5*, *43*−*46*) and that it is costly to produce sufficient amounts of protein for most of the biochemical and biophysical studies.

For the functional expression of hSGLT1 in *P. pastoris* a FLAG-tag was introduced in hSGLT1 by changing the native peptide sequence D_{574} AEEEN to D_{574}YKDDDDK. *P. pastoris* GS115 harboring a plasmid with hSGLT1 cDNA under the control of the *AOX* promoter proved to be most suitable for the high-level expression and stability of

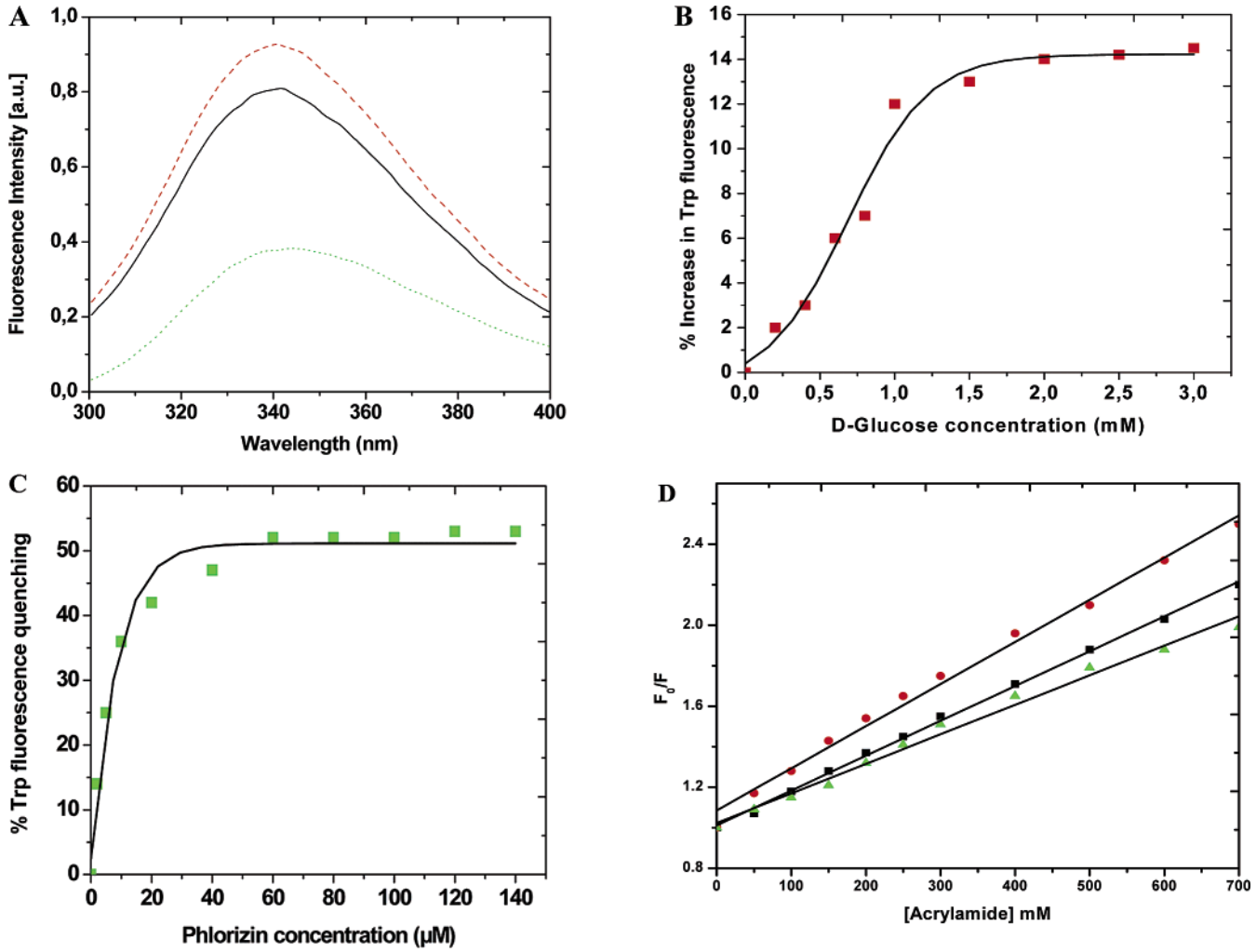

FIGURE 4: Intrinsic Trp fluorescence properties of hSGLT1. (A) Effect of D-glucose or phlorizin on the intrinsic fluorescence emission spectrum of hSGLT1. For each experiment, 4.0 μg/mL purified detergent-solubilized hSGLT1 was incubated in the absence (solid line) or presence of 10 mM D-glucose (dashed line) or in the presence of 100 μM phlorizin (dotted line). The excitation wavelength was 295 nm. The results shown are typical of ≈20 independent experiments. (B) Dose−response curve of D-glucose-induced increase in Trp fluorescence. (C) Concentration dependence of fluorescence quenching by phlorizin. (D) Effect of D-glucose (10 mM) or phlorizin (100 μM) on collisional quenching of hSGLT1 by acrylamide. Fluorescence quenching by acrylamide in the absence (■) and in the presence of 10 mM D-glucose (●) or 100 μM phlorizin (▲). Purified detergent-solubilized hSGLT1 (4.0 μg/mL) was titrated with small aliquots of stock solutions of 5 M acrylamide. The data were fitted to linear Stern−Volmer plots (see Materials and Methods), and K_{SV} values were calculated from the slope of the plots.

Table 2: The Effect of Ligands on the Trp Fluorescence of hSGLT1

ligands	max change in fluorescence (%)[a]	shifts in maxima	K_d[b] (mM)
α-MDG	+15 ± 3.5	no	0.71 ± 0.10
D-Glu	+13 ± 1	no	0.84 ± 0.15
D-Gal	+12 ± 2.3	no	0.86 ± 0.11
D-Man	+2.6 ± 0.5	no	4.5 ± 0.70
D-All	+1 ± 0.2	no	10.4 ± 1.0
L-Glu	no change	no	
Phlz	−50 ± 5	5 ± 1 (blue)	0.005 ± 0.0008

[a] Plus sign (+) indicates increase in the fluorescence intensity after addition of ligand. Minus sign (−) indicates fluorescence quenching after addition of ligand. [b] The apparent equilibrium dissociation constants (K_d) were determined with the help of eq 1 as percentage of fluorescence change as a function of ligand concentration using a computer-based analysis program (Prism). Values are the means ± SD of three independent experiments.

Table 3: Stern−Volmer Quenching Constant (K_{SV}) of hSGLT1 Fluorescence in the Presence or Absence of D-Glucose or Phlorizin

	K_{SV}[d] (M^{-1})		
quenchers	in the absence of ligand[a]	in the presence of 10 mM D-Glu[b]	in the presence of 100 μM Phlz[c]
KI	1.28 ± 0.03	1.55 ± 0.05	1.06 ± 0.03
acrylamide	1.72 ± 0.02	2.08 ± 0.05	1.46 ± 0.04
TCE	2.51 ± 0.03	3.28 ± 0.05	2.24 ± 0.05

[a] Quenching experiments were conducted in the absence of ligand. [b] Quenching experiments were conducted in the presence of 10 mM D-glucose. [c] Quenching experiments were conducted in the presence of 100 μM phlorizin. [d] The Stern−Volmer quenching constants were determined from the slopes of the lines of $F_0/F = 1 + K_{SV}[Q]$. Values are the means ± SD of three independent experiments.

recombinant hSGLT1. The transporter was detected in the yeast cells by using a FLAG antibody against the engineered FLAG epitope (Figure 2B), and it is active as judged by sodium-stimulated, secondary active sugar (α-MDG) uptake.

For the purification of hSGLT1 we adopted a new strategy, which includes washing of hSGLT1 containing membranes with 4 M urea to get rid of most of the peripheral membrane

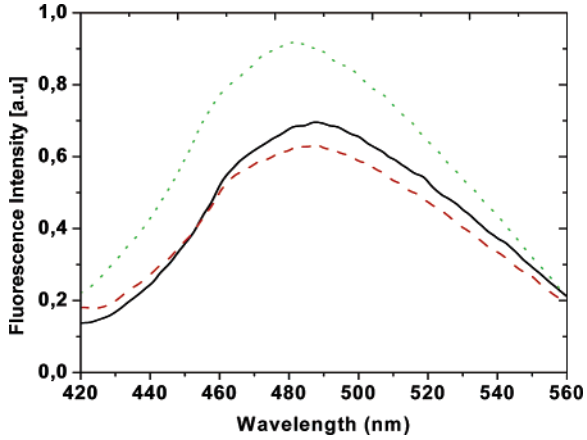

FIGURE 5: Effect of D-glucose or phlorizin on the ANS emission spectrum of hSGLT1. For each experiment, 4.0 μg/mL purified detergent-solubilized hSGLT1 labeled with 100 μM ANS was incubated in the absence (solid line) or presence of 10 mM D-glucose (dashed line) or in the presence of 100 μM phlorizin (dotted line). The excitation wavelength was 370 nm. The results shown are typical of ≈20 independent experiments.

proteins, which helps in the enrichment of hSGLT1. As judged by Western blot analysis during different stages of hSGLT1 purification, the hSGLT1 was properly inserted into the membrane because in the supernatant (Figure 2B, lane S1) and in the urea washing (Figure 2B, lane UW), we could not detect any hSGLT1 protein, all hSGLT1 was present in the pellet (Figure 2B, lane P1), and could be released into the supernatant (Figure 2B, lane S4), after solubilization of the membranes in 1.2% FosCholine-12.

A variety of motifs have been reported for the specific localization of particular membrane proteins to specific membrane compartments (*47*−*50*), but the elements that guide hSGLT1 insertion into the membrane are still unclear. Recently, Quick and Wright (*8*) observed that a shorter N-terminal of hSGLT1 increased the amount of hSGLT1 inserted into the *E. coli* membrane. However, in *P. pastoris* most of the hSGLT1 inserted into membrane without any modification at its N-terminal. These results indicate that the membrane-targeting signals encoded within the hSGLT1 sequence are fully functional in *P. pastoris.*

Purified hSGLT1 shows an apparent molecular mass of 55 kDa. This represents the nonglycosylated hSGLT1 protein as confirmed by the observation that the protein band showed no shift in electrophoretic mobility after treatment with endoglycosidase F (data not shown). Despite the lack of glycosylation the purified hSGLT1 shows properties that are indistinguishable from glycosylated hSGLT1. This finding supports previous observations that N-glycosylation is not required for hSGLT1 activity (*8*, *40*, *51*).

hSGLT1 in proteoliposomes exhibits substrate specificity in the following order: α-MDG > D-Glc ≈ D-Gal ≫ Man > All > L-Glc. The apparent K_m values for the various sugars and the stereospecificity of recombinant hSGLT1 mirror those determined for hSGLT1 in native tissue and *Xenopus* oocytes (*52*−*54*). Catalytic turnover of hSGLT1 based on the V_{max} of 3.4 μmol × mg hSGLT1^{-1} × min^{-1} is 6 s^{-1}, which is in good agreement with that obtained in previous studies (*8*) and other Na^+-dependent transporters [e.g., the Na^+/glucose transporter of *Vibrio parahaemolyticus* (vSGLT) (*25*), and Na^+/proline transporter of *Escherichia coli* (PutP) (*27*)]. We performed all transport assays in proteoliposomes at 22 °C because proteoliposomes of above lipid composition are unstable at 37 °C, however, we expect that the turnover number determined for hSGLT1 at 22 °C varies only slightly if determined at 37 °C as previous studies on temperature dependence of SGLT1 in hog renal brush border membrane vesicles carried out by De Smedt and Kinne (*55*) indicate that when increasing the temperature from 22 °C to 37 °C the turnover number increases only by 5−10%.

The current method of expression of hSGLT1 in *P. pastoris* might have certain advantages over other methods of hSGLT1 expression. We expressed full-length hSGLT1 protein only with minor modifications in hSGLT1 as compared to previously reported hSGLT1 expression in *E. coli* (*8*), in which N-terminal of hSGLT1 was shortened by deleting amino acid residues 12−28 and GFP was fused to its C-terminal. This addition might complicate the application of biochemical and biophysical methods due to the high molecular weight (≈100 kDa) of hSGLT1-Δ*N*-GFP. The amount of hSGLT1 (3 mg of hSGLT1 per 1-liter of yeast culture) obtained in our expression system is the highest yield reported so far for hSGLT1 protein expression. The yield obtained in *E. coli* was only 1 mg of purified recombinant protein per 3-liters of cultured bacterial cells.

For the better immunological detection and to facilitate the purification two affinity tags are present in the protein. The protein purification method is very simple and efficient; washing the protein pellet with 4 M urea resulted in a pellet enriched in hSGLT1 protein which was solubilized in 1.2% FosCholine-12, and the resultant solubilized supernatant gave more than 95% purified hSGLT1 protein without any degradation product after Ni-affinity purification on a Protino column.

Fluorescence Studies. The location of the maximum of the combined fluorescence of the 14 Trps present in hSGLT1 suggests that in the detergent containing solution the majority of Trps are located in a hydrophobic environment. This assumption is supported by the low accessibility of Trps to hydrophilic quenchers. Similar findings have been reported for other isolated membrane proteins such as the Na^+/galactose cotransporter of *Vibrio parahaemolyticus* (acrylamide Ksv = 2.6 M^{-1}) (*56*), lactose permease of *E. coli* (KI Ksv = 1.12 M^{-1} and acrylamide Ksv = 2.01 M^{-1}) (*57*), P-glycoprotein multidrug transporter (acrylamide Ksv = 2.6 M^{-1}) (*58*), and Ca^{2+}-ATPase (acrylamide Ksv = 1.9 M^{-1}) (*59*).

Based on topology predictions the N-terminal half of hSGLT1 contains nine Trps, and the C-terminal half contains five residues. Seven residues in the N-half (Trp 45, Trp 66 and 67, Trp103 and 114, and Trp 289 and 291) are located within putative TM segments 1, 2, 3, and 7, respectively. Trp 6 is positioned in the extracellular N-terminal tail and Trp 276 in an extracellular loop. Four residues in the C-half (Trp 440, Trp 477, Trp 487, and Trp 641) are found in putative TM segments 10, 11, 12, and 14, respectively. Trp 561 is located in the intracellular/extracellular loop13. Thus the majority of the Trps (11 out of 14) are predicted to be in a hydrophobic environment; this seems to be the case also in the experimental conditions used in this study.

The presence of D-glucose in the medium induces significant changes in the experimental parameters. The sugar increases the intrinsic fluorescence of the protein. Interest-

ingly, the interaction with D-glucose is a saturable process with an apparent affinity constant of 0.84 ± 0.15 mM, which is an affinity in the same range as observed in transport studies. In addition, the binding exhibited a stereospecificity that is also very similar to the stereospecificity found for sugar translocation through the carrier. It is further noteworthy that all the above changes are only observed in the presence of sodium. In solution it is possible that hSGLT1 exists in two orientations, right-side-out (RSO) or inside-out (ISO) as reported for sugar phosphate transporter (UhpT) of *Escherichia coli* (*60*). Sodium-dependence, stereospecificity, and affinity of D-glucose however provide strong evidence that the binding occurs to the extracellular side of the transporter (*40*, *61*). The internal binding site as deduced from transport studies on inside-out orientated membrane vesicles is sodium independent and has a much lower D-glucose affinity and also a different stereospecificity (*40*). In addition the transport is phlorizin insensitive. Furthermore in the reconstituted proteoliposomes hSGLT1 exhibited similar ligand and inhibitor induced fluorescence changes in the presence of sodium (data not shown). These results strongly suggest that the fluorescence changes we observe in solution arise due to binding of ligands at the extracellular face of hSGLT1. The dose−response curve in Figure 4B for D-glucose yields a Hill coefficient 1.4, which might indicate that hSGLT1 contains more than one D-glucose binding site at the external surface and that these sites exert positive cooperativity. Results from our group (Kumar and Kinne, unpublished data) and Wright et al. (*62*) also indicate the presence of two sugar-binding sites.

The increased fluorescence of the sugar−SGLT1 complex can most easily be explained by a conformational change where some Trps became exposed to a more hydrophilic environment, which makes them more accessible to hydrophilic collisional quenchers. The observed ANS fluorescence indicates an increased hydrophilicity also of the surface of the protein. Whether the same Trps are part of the sugar binding/transport pathway is not clear; to answer this question Trp scanning mutagensis studies are underway in our group. The increased accessibility might also result from conformational changes at parts other than the sugar-binding site of the protein. One possibility would be the sodium-binding site. In transport and fluorescence studies a tight conformational coupling between the sugar binding site and sodium binding sites has been predicted (*63*).

Phlorizin is a high affinity inhibitor of SGLT1, which is supposed to interact on one hand with the D-glucose binding site and on the other hand with an additional aglucone-binding site of the transporter. Several studies have shown by kinetic analysis and by single molecule recognition atomic force microscopy that these interactions occur at the extracellular face of SGLT1 (*64*), suggesting a similar situation in the in vitro studies described here. Also the sodium-dependence and the high affinity of the inhibition provide evidence for this assumption. At the intracellular face of SGLT1 a very low affinity (if at all) for sodium and phlorizin has been described (*40*).

Phlorizin led to a striking reduction of the intrinsic fluorescence with a strong blue shift and exhibited a slight protection against hydrophilic collisional quenchers and an increase of hydrophobicity on the outer surface of transporter. The reduction of the fluorescence could indicate that phlorizin was in close contact with Trps, which leads to quenching. In vitro studies on isolated functional domains in solution revealed strong conformational changes in loop 13 that were related to phlorizin binding to the peptide and induced reduction in Trp fluorescence (*9*, *10*). The increase in hydrophobicity at the outer surface of the protein points to the formation of a more occluded state of the protein. This could be the result of a reorientation of the transmembrane helices, caused by the distinct changes in topology in the surface loops of the protein described previously by single molecule recognition atomic force microscopy (*64*).

On the basis of the results presented above we can distinguish between three different conformational states of SGLT1. The empty carrier (conformational state "C") exhibits a relatively medium intensity of intrinsic fluorescence, ANS fluorescence, and a low accessibility of the Trps to collisional quenchers. The sugar-loaded transporter (conformational state "CNa_2S") shows the highest intensity in intrinsic fluorescence, a low ANS fluorescence, and an increased accessibility of the Trps to collisional quenchers. This less compact, probably more flexible, conformation might prepare the protein to execute the transmembrane translocation of the sugar and sodium ions. The phlorizin-loaded carrier (conformational state "CNa_2Pz") on the other hand shows the lowest intrinsic fluorescence and a strongly increased ANS fluorescence. Thus phlorizin inhibits sugar transport not only by competing with the sugar at the sugar-binding site as assumed previously but in addition transfers to the protein a more compact probably more rigid conformation, thus making translocation of sugars impossible. This assumption is supported by the fact that in transport studies in right-side-out orientated vesicles phlorizin when present in the incubation medium (outside the vesicles) inhibits sugar efflux from the inside of the vesicles (*65*).

Interestingly, we were not able to detect conformational changes of hSGLT1 induced by Na^+ (conformational state "CNa_2"). This might be due to the fact that after interaction with Na^+ hSGLT1 undergoes conformational changes in which microenvironments of Trp residues do not change. Existence of three different conformational states of hSGLT1 was also reported in *Xenopus* oocytes (*24*, *63*) by electrophysiology. Our intrinsic and extrinsic fluorescence data identified phlorizin bound transporter (conformational state "CNa_2Pz") which was not reported in the literature up to this date.

In summary, this study provides the first example of large-scale functional expression and purification of full-length human Na^+/D-glucose cotransporter1. Recombinant hSGLT1 retains full functionalities when reconstituted into proteoliposomes. Spectroscopic studies of hSGLT1 in solution identify different conformational states of protein in the presence or absence of ligand. We hope that hSGLT1 protein obtained by this method will provide a starting point for different biochemical and biophysical experiments, which provide insight into different conformations of hSGLT1 and the mechanism of sugar transport.

ACKNOWLEDGMENT

We thank Deutsches Ressourcenzentrum für Genomforschung GmbH (RZPD, Berlin, Germany) for providing DKFZp686N20230Q2 clone containing full-length hSGLT1

gene. We are indebted to Dr. Rana Roy for giving his valuable advice for hSGLT1 expression and purification. We are thankful for support from the International Max Planck Research School in Chemical Biology, Dortmund, Germany (N.K.T.), the August-Lenz-Stiftung and the Deutsche Forschungsgemeinschaft (Graduate Program "Vascular Biology in Medicine" GRK438 (P.G.), SFB 413 and Si 274/9.

REFERENCES

1. International Human Genome Sequencing Consortium. (2001) *Nature 409*, 860−921.
2. Hediger, M. A., Coady, M. J., Ikeda, T. S., and Wright, E. M. (1987) Expression cloning and cDNA sequencing of the Na^+/glucose cotransporter, *Nature 330*, 379−381.
3. Pajor, A. M., and Wright, E. M. (1992) Cloning and functional expression of a mammalian Na^+/nucleoside cotransporter. A member of the SGLT family, *J. Biol. Chem. 267*, 3557−3560.
4. Turk, E., Zabel, B., Mundlos, S., Dyer, J., and Wright, E. M. (1991) Glucose/galactose malabsorption caused by a defect in the Na^+/glucose cotransporter, *Nature 350*, 354−356.
5. Birnir, B., Lee, L. S., Hediger, M. A., and Wright, E. M. (1990) Expression and characterization of the intestinal Na^+/glucose cotransporter in COS-7 cells, *Biochim. Biophys. Acta 1048*, 100−104.
6. Smith, C. D., Hirayama, A., and Wright, E. M. (1992) Baculovirus-mediated expression of the Na^+/glucose cotransporter in Sf9 cells, *Biochim. Biophys. Acta 1104*, 151−159.
7. Lin, J. T., Kormanec, J., Wehner, F., Wielert-Badt, S., and Kinne, R. K. H. (1998) High-level expression of Na^+/D-glucose cotransporter (SGLT1) in a stably transfected Chinese hamster ovary cell line, *Biochim. Biophys. Acta 1373*, 309−320.
8. Quick, M., and Wright, E. M. (2002) Employing *Escherichia coli* to functionally express, purify, and characterize a human transporter, *Proc. Natl. Acad. Sci. U.S.A. 99*, 8597−8601.
9. Xia, X., Lin, J. T., and Kinne, R. K. H. (2003) Binding of phlorizin to the isolated C-terminal extramembranous loop of the Na^+/glucose cotransporter assessed by intrinsic tryptophan fluorescence, *Biochemistry 42*, 6115−6120.
10. Raja, M. M., Tyagi, N. K., and Kinne, R. K. H. (2003) Phlorizin recognition in a C-terminal fragment of SGLT1 studied by tryptophan scanning and affinity labeling, *J. Biol. Chem. 278*, 49154−49163.
11. Tyagi, N. K., and Kinne, R. K. H. (2003) Synthesis of photoaffinity probes [2′-4′-iodo-(3″-trifluoromethyldiazirinyl)phenoxy]-D-glucopyranoside and [(4′-benzoyl)phenoxy]-D-glucopyranoside for the identification of sugar-binding and phlorizin-binding sites in the sodium/D-glucose cotransporter protein, *Anal. Biochem. 323*, 74−83.
12. Raja, M. M., Kipp, H., and Kinne, R. K. H. (2004) C-terminus loop 13 of Na^+ glucose cotransporter SGLT1 contains a binding site for alkyl glucosides, *Biochemistry 43*, 10944−10951.
13. Cereghino, J. L., and Cregg, J. M. (2000) Heterologous protein expression in the methylotrophic yeast *Pichia pastoris*, *FEMS Microbiol. Rev. 24*, 45−66.
14. Lang, C., and Bottner, M. (2004) High-throughput expression in microplate format in *Pichia pastoris*, *Methods Mol. Biol. 267*, 277−286.
15. Cregg, J. M., Cereghino, J. L., Shi, J., and Higgins, D. R. (2000) Recombinant protein expression in *Pichia pastoris*, *Mol. Biotechnol. 16*, 23−52.
16. Higgins, D. R., and Cregg, J. M. (1998) *Methods in Molecular Biology: Pichia Protocols*, Vol. 103, Humana Press, Totowa, NJ.
17. Strugatsky, D., Gottschalk, K. E., Goldshleger, R., Bibi, E., and Karlish, S. J. D. (2003) Expression of Na^+, K^+-ATPase in *Pichia pastoris*: analysis of wild type and D369N mutant proteins by Fe^{2+}-catalyzed oxidative cleavage and molecular modeling, *J. Biol. Chem. 278*, 46064−46073.
18. Cai, J., Daoud, R., Georges, E., and Gros, P. (2001) Functional expression of multidrug resistance protein 1 in *Pichia pastoris*, *Biochemistry 40*, 8307−8316.
19. Cai, J., and Gros, P. (2003) Overexpression, purification, and functional characterization of ATP-binding cassette transporters in the yeast, *Pichia pastoris*, *Biochim. Biophys. Acta 1610*, 63−76.
20. Bieszke, J. A., Spudich, E. N., Scott, K. L., Borkovich, K. A., and Spudich, J. L. (1999) A eukaryotic protein, anop-1, binds retinal to form an archaeal rhodopsin-like photochemically reactive pigment, *Biochemistry 38*, 14138−14145.
21. Doring, F., Theis, S., and Daniel, H. (1997) Expression and functional characterization of the mammalian intestinal peptide transporter pepT1 in methylotrophic yeast *Pichia pastoris*, *Biochem. Biophys. Res. Comm. 232*, 656−662.
22. Talmont, F., Sidobre, S., Demange, P., Milion, A., and Emorine, L. J. (1996) Expression and pharmacological characterization of the human mu-opioid receptor in the methylotrophic yeast *Pichia pastoris*, *FEBS Lett. 394*, 268−272.
23. Weiss, H. M., Haase, W., and Reilander, H. (1998) Expression of an integral membrane protein, the $5HT_{5A}$ receptor, *Methods Mol. Biol. 103*, 227−239.
24. Loo, D. D. F., Hirayama, B. A., Gallardo, E. M., Lam, J. T., Turk, E., and Wright, E. M. (1998) Conformational changes couple Na^+ and glucose transport, *Proc. Natl. Acad. Sci. U.S.A. 95*, 7789−7794.
25. Turk, E., Kim, O., Le Courte, J., Whitelegge, J. P., Eskandari, S., Lam, J. T., Kreman, M., Zampighi, G. A., Faull, K. F., and Wright, E. M. (2000) Molecular characterization of *Vibrio parahaemolyticus* Vsglt: a model for sodium-coupled sugar cotransporters, *J. Biol. Chem. 275*, 25711−25716.
26. Sambrook, J., Fritsch, E. F., and Maniatis, T. (2001) *Molecular Cloning: A Laboratory Manual*, 3rd ed., Cold Spring Harbor Laboratory, Cold Spring Harbor, NY.
27. Jung, H., Tebbe, S., Schmid, R., and Jung, K. (1998) Unidirectional reconstitution and characterization of purified Na^+/proline transporter of *Escherichia coli*, *Biochemistry 37*, 11083−11088.
28. Panayotova-Heiermann, M., Leung, D. W., Hirayama, B. A., and Wright, E. M (1999) Purification and functional reconstitution of a truncated human Na^+/glucose cotransporter (SGLT1) expressed in *E. coli*, *FEBS Lett. 459*, 386−390.
29. Rigaud, J.-L., and Daniel, L. (2003) Reconstitution of membrane proteins into liposomes, *Methods Enzymol. 372*, 65−86.
30. Rigaud, J.-L., Pitard, B., and Daniel, L. (1995) Reconstitution of membrane proteins into liposomes: application to energy-transducing membrane proteins, *Biochim. Biophys. Acta 1231*, 223−246.
31. Holloway, P. W. (1973) A simple procedure for removal of Triton X-100 from protein samples, *Anal. Biochem. 53*, 304−308.
32. Laemmli, U. K. (1970) Cleavage of structural proteins during the assembly of the head of bacteriophage T4, *Nature 227*, 680−685.
33. Blum, H., Beier, H., and Gross, H. J. (1987) Improved silver staining of plant proteins, RNA and DNA in polyacrylamide gels, *Electrophoresis 8*, 93−99.
34. Daniel, E., and Weber, G. (1966) Cooperative effects in binding by bovine serum albumin. I. The binding of 1-anilino-8-naphthalenesulfonate. Fluorimetric titrations, *Biochemistry 5*, 1893−1900.
35. Romanos, M. A., Scorer, C. A., Sreekrishna, K., and Clare, J. (1998) The generation of multicopy recombinant strains, *Methods Mol. Biol. 103*, 55−72.
36. Scorer, C. A., Buckholz, R. G., Clare, J. J., and Romanos, M. A. (1993) The intracellular production and secretion of HIV-1 envelope protein in the methylotrophic yeast *Pichia pastoris*, *Gene 136*, 111−119.
37. Kinne, R. (1976) Properties of the glucose transport system in the renal brush border membrane, *Curr. Top. Membr. Trans. 8*, 209−268.
38. Lücke, H., Berner, W., Menge, H., and Murer, H. (1978) Sugar transport by brush border membrane vesicles isolated from human small intestine, *Pfluegers Arch. 373*, 243−248.
39. Diez-Sampedro, A., Wright, E. M., and Hirayama, B. A. (2001) Residue 457 controls sugar binding and transport in the Na^+/glucose cotransporter, *J. Biol. Chem. 276*, 49188−49194.
40. Fringes, M. A., Lin, J. T., and Kinne, R. K. H. (2001) Functional asymmetry of the sodium-D-glucose cotransporter expressed in yeast secretory vesicles, *J. Membr. Biol. 179*, 143−153.
41. Napoli, R., Hirshman, M. F., and Horton, E. S. (1995) Mechanisms and time course of impaired skeletal muscle glucose transport activity in streptozocin diabetic rates, *J. Clin. Invest. 96*, 1−11.
42. King, P. A., Betts, J. J., Horton, E. D., and Horton, E. S. (1993) Exercise, unlike insulin, promotes glucose transporter translocation in obese Zucker rat muscle, *Am. J. Physiol. 265*, R447−R452.
43. Lostao, M. P., Hirayama, B. A., Panayotova-Heiermann, M., Sampogna, S. L., Bok, D., and Wright, E. M. (1995) Arginine-427 in the Na^+/glucose cotransporter (SGLT1) is involved in trafficking to the plasma membrane, *FEBS Lett. 377*, 181−184.

44. Martin, M. G., Turk, E., Lostao, M. P., Kerner, C., and Wright, E. M. (1996) Defects in Na^+/glucose cotransporter (SGLT1) trafficking and function cause glucose-galactose malabsorption, *Nat. Genet. 12*, 216−220.
45. Martin, M. G., Lostao, M. P., Turk, E., Lam, J., Kreman, M., and Wright, E. M. (1997) Compound missense mutations in the sodium/D-glucose cotransporter result in trafficking defects, *Gastroenterology 112*, 1206−1212.
46. Lam, J. T., Martin, M. G., Turk, E., Hirayama, B. A., Bosshard, N. U., Steinmann, B., and Wright, E. M. (1999) Missense mutations in SGLT1 cause glucose-galactose malabsorption by trafficking defects, *Biochim. Biophys. Acta 1453*, 297−303.
47. Bibi, E., Stearns, S. M., and Kaback, H. R. (1992) The N-terminal 22 amino acid residues in the lactose permease of *Escherichia coli* are not obligatory for membrane insertion or transport activity, *Proc. Natl. Acad. Sci. U.S.A. 89*, 3180−3184.
48. Weinglass, A. B., and Kaback, H. R. (2000) The central cytoplasmic loop of the major facilitator superfamily of transport proteins governs efficient membrane insertion, *Proc. Natl. Acad. Sci. U.S.A. 97*, 8938−8943.
49. Matter, K., Hunziker, W., and Mellman, I. (1992) Basolateral sorting of LDL receptor in MDCK cells: the cytoplasmic domain contains two tyrosine-dependent targeting determinants, *Cell 71*, 741−753.
50. Sandoval, I. V., and Bakke, O. (1994) Targeting of membrane proteins to endosomes and lysosomes, *Trends Cell Biol. 4*, 292−297.
51. Turk, E., Kerner, C. J., Loasto, M. P., and Wright, E. M. (1996) Membrane topology of the human Na^+/glucose cotransporter SGLT1, *J. Biol. Chem. 271*, 1925−1934.
52. Diedrich, D. F. (1966) Competitive inhibition of intestinal glucose transport by phlorizin analogs, *Arch. Biochem. Biophys. 117*, 248−256.
53. Schultz, S. G., and Curran, P. F. (1970) Coupled transport of sodium and organic solutes, *Physiol. Rev. 50*, 637−718.
54. Ikeda, T. S., Hwang, E. S., Coady, M. J., Hirayama, B. A., Hediger, M. A., and Wright, E. M. (1989) Characterization of a Na^+/glucose cotransporter cloned from rabbit small intestine, *J. Membr. Biol. 110*, 87−95.
55. De Smedt, H., and Kinne, R. (1981) Temperature dependence of solute transport and enzyme activities in hog renal brush border membrane vesicles, *Biochim. Biophys. Acta 648*, 247−253.
56. Veenstra, M., Turk, E., and Wright, E. M. (2002) A ligand dependent conformational change of the Na^+/galactose cotransporter of *Vibrio parahaemolyticus*, monitored by tryptophan fluorescence, *J. Membr. Biol. 185*, 249−255.
57. Vazquez-Ibar, J. L., Guan, L., Svrakic, M., and Kaback, H. R. (2003) Exploiting luminescence spectroscopy to elucidate the interaction between sugar and tryptophan residue in the lactose permease of *Escherichia coli*, *Proc. Natl. Acad. Sci. U.S.A. 100*, 12706−12711.
58. Liu, R., Siemiarczuk, A., and Sharom, F. J. (2000) Intrinsic fluorescence of the P-glycoprotein multidrug transporter: sensitivity of tryptophan residues to binding of drugs and nucleotides, *Biochemistry 39*, 14927−14938.
59. Gryczynski, I., Wiczk, W., Inesi, G., Squier, T., and Lakowicz, J. R. (1989) Characterization of the tryptophan fluorescence from sarcoplasmic reticulum adenosine triphosphatase by frequency-domain fluorescence spectroscopy, *Biochemistry 28*, 3490−3498.
60. Fann, M.-C., and Maloney, P. C. (1998) Functional symmetry of UheT, the sugar phosphate transporter of *Escherichia coli*, *J. Biol. Chem. 273*, 33735−33740.
61. Quick, M., Tomasevic, J., and Wright, E. M. (2003) Functional asymmetry of the human Na^+/glucose cotransporter (hSGLT1) in bacterial membrane vesicles, *Biochemistry 42*, 9147−9152.
62. Wright, E. M., Loo, D. D. F., Hirayama, B. A., and Turk, E. (2004) Surprising Versatility of Na^+-Glucose Cotransporters: SLC5, *Physiology 19*, 370−376.
63. Meinild, A.-K., Hirayama, B. A., Wright, E. M., and Loo, D. D. F. (2002) Fluorescence studies of ligand-induced conformational changes of the Na^+/glucose cotransporter, *Biochemistry 41*, 1250−1258.
64. Wielert-Badt, S., Hinterdorfer, P., Gruber, H. J., Lin, J. T., Badt, D., Wimmer, B., Schindler, H., and Kinne, R. K. (2002) Single molecule recognition of protein binding epitopes in brush border membranes by force microscopy, *Biophys. J. 82*, 2767−2774.
65. Kinne, R., Murer, H., Kinne-Saffran, E., Thees, M., and Sachs, G. (1975) Sugar transport by renal plasma membrane vesicles, *J. Membr. Biol. 21*, 375−395.

BI051377Q